Leading order relativistic hyperon-nucleon interactions in chiral effective field theory[*]

Kai-Wen Li(李凯文)[1]   Xiu-Lei Ren(任修磊)[2]   Li-Sheng Geng(耿立升)[1,3;1]   Bing-Wei Long(龙炳蔚)[4]

[1] School of Physics and Nuclear Energy Engineering and International Research Center for Nuclei and Particles in the Cosmos, Beihang University, Beijing 100191, China

[2] School of Physics and State Key Laboratory of Nuclear Physics and Technology, Peking University, Beijing 100871, China

[3] Beijing Key Laboratory of Advanced Nuclear Materials and Physics, Beihang University, Beijing 100191, China

[4] Center for Theoretical Physics, Department of Physics, Sichuan University, 29 Wang-Jiang Road, Chengdu, Sichuan 610064, China

Abstract: We apply a recently proposed covariant power counting in nucleon-nucleon interactions to study strangeness $S=-1$ $\Lambda N-\Sigma N$ interactions in chiral effective field theory. At leading order, Lorentz invariance introduces 12 low energy constants, in contrast to the heavy baryon approach, where only five appear. The Kadyshevsky equation is adopted to resum the potential in order to account for the non-perturbative nature of hyperon-nucleon interactions. A fit to the 36 hyperon-nucleon scattering data points yields $\chi^2 \simeq 16$, which is comparable with the sophisticated phenomenological models and the next-to-leading order heavy baryon approach. However, one cannot achieve a simultaneous description of the nucleon-nucleon phase shifts and strangeness $S=-1$ hyperon-nucleon scattering data at leading order.

1   Introduction

Since the quantum number *strangeness* was introduced [1, 2] and the first observation of Λ hypernuclei [3] in 1953, strangeness nuclear physics has always been at the frontier of experimental and theoretical nuclear physics. In recent years, open questions such as charge symmetry breaking in $A=4$ Λ-hypernuclei [4] and the existence of the H-dibaryon [5] have attracted a lot of attention [6–11]. In facilities like JLab, J-PARC, KEK, MAMI, and COSY, many important studies are being pursued, e.g., the level spectra and decay properties of Λ, double Λ and Ξ hypernuclei [12–16], Σp scattering [17], and final state interactions in production reactions, such as $\vec{p}p \to K^+\Lambda p$ [18], which can provide information on the ΛN scattering lengths. Meanwhile, theoretical few- and many-body calculations of hypernuclei have made steady progress, see, e.g., Refs. [19, 20]. One particularly interesting ongoing issue is about the role of hyperons in the cores of neutron stars, known as the *hyperon puzzle*: nuclear many-body calculations incorporating hyperon degrees of freedom [21–25] have difficulties in obtaining a two-solar mass neutron star that was recently observed [26, 27].

As the most important theoretical input for few- and many-body calculations, baryon-baryon interactions play an indispensable role in studies of hypernuclear physics. Although many efforts have been made to derive them, previous theoretical investigations were mainly based on phenomenological meson-exchange models [28–35] and quark models [36–42]. In the past two decades, two breakthroughs have occurred in constructing model-independent baryon-baryon interactions. Both of them are closely related to quantum chromodynamics (QCD), the underlying theory of strong interactions. One breakthrough is lattice QCD simulations [43–48], which provide an *ab initio* numerical solution to QCD from first principles. With ever-growing computing power and evolving numerical algorithms, lattice QCD simulations are approaching the physical world [49, 50], thus providing us with more information and constraints on baryon-baryon interactions. The other is chiral effective field theory (χEFT), which has achieved great successes in nucleon-nucleon (NN) interactions [51–53] following Weinberg's proposal [54, 55]. The latter approach has been generalized to antinucleon-nucleon [56], hyperon-nucleon (YN) [57–59] and multi-strangeness systems [60–62]. The main advantage of χEFT is that by using a

power counting scheme, one can improve calculations systematically by going to higher orders in powers of external momenta and light quark masses, and estimating the uncertainties of any given order. Furthermore, three- and four-body forces automatically arise as we push through the hierarchy of chiral forces.

However, the Weinberg approach for baryon-baryon interactions, denoted as the heavy baryon (HB) approach, is based on a non-relativistic formalism. It is sensitive to ultraviolet cutoffs, that is, renormalization group invariance is violated, risking severe model dependence of short-range physics. Various opinions on this issue can be found in Refs. [63–70]. In two recent papers, Epelbaum and Gegelia have proposed a new approach (referred to as the EG approach in the present paper) to NN scattering in χEFT [71, 72], where the relativistic effects are partially retained. At leading order (LO), the potential remains unchanged but the scattering equation changes to the Kadyshevsky equation, compared to the Lippmann-Schwinger equation with nonrelativistic nucleon propagators in the HB approach. Although this turned out to describe the Nijmegen partial wave analysis [73] well, a higher order contact term is still needed in the $^3P_0$ partial wave to achieve renormalization group invariance. We applied the EG approach to the strangeness $S=-1$ YN system [74] and found that the best description of the experimental data is quantitatively similar to that of the HB approach, and that cutoff dependence is mitigated but not removed.

Partly motivated by the successes of covariant χEFT in the one-baryon and heavy-light systems [75–83], a new covariant power counting is explored in Ref. [84] to study NN chiral interactions. The covariant treatment of baryons maintains all the symmetries and analyticities, and, at LO, it results in a description of the NN phase shifts similar to that of the next-to-leading order (NLO) HB scheme. In the present study, we apply this scheme to YN scattering with strangeness $S=-1$, where more particle channels and less experimental data should be dealt with.

2 Formalism

2.1 Covariant power counting

First, we explain in some detail the covariant power counting scheme proposed in Ref. [84][1]. Unlike the meson-meson and meson-baryon sectors, such a power counting in the baryon-baryon sector is not yet systematically formulated beyond leading order. In particular, relativistic contact baryon-baryon interactions should be treated carefully, see, e.g. Ref. [85]. In the covariant scheme, one takes the full Dirac spinors for the baryon fields and uses partial derivatives on the baryon/meson

fields and meson mass insertions to increase the chiral order.

The perturbative expansion is consistent with conventional χEFT, in which the scattering amplitude is expanded in terms of a small quantity over a large quantity. The former could be the meson momentum or mass, or the baryon three-momenta, and the latter could be the ρ meson mass or the nucleon mass or the chiral symmetry breaking scale. In Ref. [84], naive dimensional analysis is used to determine the chiral order ν,

$$\nu=2-\frac{1}{2}B+2L+\sum_i v_i\Delta_i, \qquad \Delta_i=d_i+\frac{1}{2}b_i-2, \qquad (1)$$

where B denotes the number of external baryons, L is the number of Goldstone boson loops and v_i is the number of vertices with dimension Δ_i. For a vertex with dimension Δ_i, d_i is the number of derivatives or Goldstone boson masses, and b_i is the number of internal baryon lines.

At leading order, there are no derivatives or pseudoscalar meson mass insertions. Therefore, the complete structures are determined by the Clifford algebra (Γ_i), namely the five Lorentz structures shown in the following section. These five structures have been derived in a number of early studies in the nucleon-nucleon sector [57, 85, 86]. Some authors consider the terms involving only γ_5 as higher order because they connect the large and small components of the Dirac spinors [87]. In our present case, we do not expand the Dirac spinors and therefore retain them.

2.2 Leading order baryon-baryon interactions

In covariant power counting [84], the full baryon spinor is retained to maintain Lorentz invariance

$$u_B(\boldsymbol{p},s)=N_p\left(\begin{array}{c}1\\ \frac{\boldsymbol{\sigma}\cdot\boldsymbol{p}}{E_p+M_B}\end{array}\right)\chi_s, \quad N_p=\sqrt{\frac{E_p+M_B}{2M_B}}, \quad (2)$$

where $E_p=\sqrt{\boldsymbol{p}^2+M_B^2}$, while a non-relativistic reduction of u_B is employed in the HB approach. The LO baryon-baryon interactions include non-derivative four-baryon contact terms (CT) and one-pseudoscalar-meson exchange (OPME) potentials, as shown in Fig. 1,
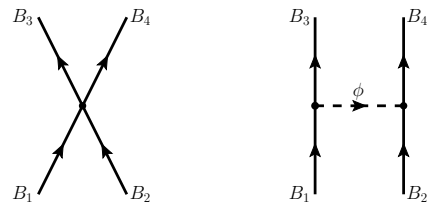

Fig. 1. Non-derivative four-baryon contact terms and OPME at LO. The solid lines denote incoming and outgoing baryons ($B_{1,2,3,4}$), and the dashed line denotes the exchanged pseudoscalar meson ϕ.

---

1) See, also, Refs.[85, 86] for early attempts.

$$V_{\mathrm{LO}} = V_{\mathrm{CT}} + V_{\mathrm{OPME}}. \qquad (3)$$

2.2.1 Four-baryon contact terms

The Lagrangian term for non-derivative four-baryon contact interactions [57] is

$$\mathcal{L}_{\mathrm{CT}} = \sum_{i=1}^{5} \left[\frac{\tilde{C}_i^1}{2}\, \mathrm{tr}\left(\bar{B}_1 \bar{B}_2 (\Gamma_i B)_2 (\Gamma_i B)_1\right) \right.$$
$$+ \frac{\tilde{C}_i^2}{2}\, \mathrm{tr}\left(\bar{B}_1 (\Gamma_i B)_1 \bar{B}_2 (\Gamma_i B)_2\right)$$
$$\left. + \frac{\tilde{C}_i^3}{2}\, \mathrm{tr}\left(\bar{B}_1 (\Gamma_i B)_1\right) \mathrm{tr}\left(\bar{B}_2 (\Gamma_i B)_2\right) \right], \qquad (4)$$

where tr indicates the trace in flavor space (u, d, and s). Only baryon fields with the same subscript, 1 or 2, are grouped to form a Lorentz-covariant bilinear. Γ_i are the elements of the Clifford algebra,

$$\Gamma_1 = 1, \quad \Gamma_2 = \gamma^\mu, \quad \Gamma_3 = \sigma^{\mu\nu}, \quad \Gamma_4 = \gamma^\mu \gamma_5, \quad \Gamma_5 = \gamma_5; \quad (5)$$

and $\tilde{C}_i^m$ ($m=1,2,3$) are the LECs corresponding to independent four-baryon operators. The ground-state octet baryons are collected in the 3×3 traceless matrix:

$$B = \begin{pmatrix} \dfrac{\Sigma^0}{\sqrt{2}} + \dfrac{\Lambda}{\sqrt{6}} & \Sigma^+ & p \\[2mm] \Sigma^- & -\dfrac{\Sigma^0}{\sqrt{2}} + \dfrac{\Lambda}{\sqrt{6}} & n \\[2mm] \Xi^- & \Xi^0 & -\dfrac{2\Lambda}{\sqrt{6}} \end{pmatrix}. \qquad (6)$$

The Pauli exclusion principle applies; therefore, the two-baryon wave function is antisymmetric with respect to angular momentum L, spin S and flavor. The flavor symmetric and flavor antisymmetric interactions are treated differently by using Fierz rearrangements, as has been done in Ref. [57]. The resulting Lagrangians for strangeness $S = -1$ YN system in the isospin basis are shown in the following, corresponding to the three Feynman diagrams shown in Fig. 2.
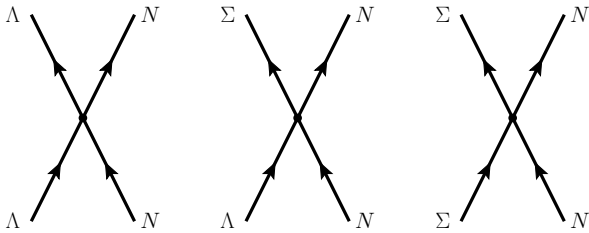

Fig. 2. The non-derivative four baryon contact terms in the $\Lambda N - \Sigma N$ system.

1) The Lagrangians for the isospin $I=1/2$ $\Lambda N \to \Lambda N$ reaction are:

$$\mathcal{L}_{1/2,\mathrm{FS}}^{\Lambda\Lambda} = \left(\frac{1}{6}C_i^1 + \frac{5}{3}C_i^2 + 2C_i^3\right)\left(\bar{\Lambda}\Gamma_i\Lambda\right)\left(\bar{N}\Gamma_i N\right)$$
$$\equiv C_{i,1/2,\mathrm{FS}}^{\Lambda\Lambda}\left(\bar{\Lambda}\Gamma_i\Lambda\right)\left(\bar{N}\Gamma_i N\right), \qquad (7)$$

$$\mathcal{L}_{1/2,\mathrm{FA}}^{\Lambda\Lambda} = \left(\frac{3}{2}C_i^1 + C_i^2 + 2C_i^3\right)\left(\bar{\Lambda}\Gamma_i\Lambda\right)\left(\bar{N}\Gamma_i N\right)$$
$$\equiv C_{i,1/2,\mathrm{FA}}^{\Lambda\Lambda}\left(\bar{\Lambda}\Gamma_i\Lambda\right)\left(\bar{N}\Gamma_i N\right), \qquad (8)$$

where the subscripts FS and FA are short for flavor symmetric (e.g., $^1S_0$, $^3P_{0,1,2}$...) and flavor antisymmetric (e.g., $^3S_1$, $^1P_1$...), respectively.

2) The Lagrangians for the isospin $I=3/2$ $\Sigma N \to \Sigma N$ reaction are:

$$\mathcal{L}_{3/2,\mathrm{FS}}^{\Sigma\Sigma} = 2(C_i^2 + C_i^3)\left(\bar{\Sigma}\Gamma_i\Sigma\right)\left(\bar{N}\Gamma_i N\right)$$
$$\equiv C_{i,3/2,\mathrm{FS}}^{\Sigma\Sigma}\left(\bar{\Sigma}\Gamma_i\Sigma\right)\left(\bar{N}\Gamma_i N\right), \qquad (9)$$

$$\mathcal{L}_{3/2,\mathrm{FA}}^{\Sigma\Sigma} = -2(C_i^2 - C_i^3)\left(\bar{\Sigma}\Gamma_i\Sigma\right)\left(\bar{N}\Gamma_i N\right)$$
$$\equiv C_{i,3/2,\mathrm{FA}}^{\Sigma\Sigma}\left(\bar{\Sigma}\Gamma_i\Sigma\right)\left(\bar{N}\Gamma_i N\right). \qquad (10)$$

3) The Lagrangians for the isospin $I=1/2$ $\Sigma N \to \Sigma N$ reaction are:

$$\mathcal{L}_{1/2,\mathrm{FS}}^{\Sigma\Sigma} = \left(\frac{3}{2}C_i^1 - C_i^2 + 2C_i^3\right)\left(\bar{\Sigma}\Gamma_i\Sigma\right)\left(\bar{N}\Gamma_i N\right)$$
$$\equiv C_{i,1/2,\mathrm{FS}}^{\Sigma\Sigma}\left(\bar{\Sigma}\Gamma_i\Sigma\right)\left(\bar{N}\Gamma_i N\right)$$
$$= \left(9C_{i,1/2,\mathrm{FS}}^{\Lambda\Lambda} - 8C_{i,1/2,\mathrm{FS}}^{\Sigma\Sigma}\right)\left(\bar{\Sigma}\Gamma_i\Sigma\right)\left(\bar{N}\Gamma_i N\right), \quad (11)$$

$$\mathcal{L}_{1/2,\mathrm{FA}}^{\Sigma\Sigma} = \left(\frac{3}{2}C_i^1 + C_i^2 + 2C_i^3\right)\left(\bar{\Sigma}\Gamma_i\Sigma\right)\left(\bar{N}\Gamma_i N\right)$$
$$\equiv C_{i,1/2,\mathrm{FA}}^{\Sigma\Sigma}\left(\bar{\Sigma}\Gamma_i\Sigma\right)\left(\bar{N}\Gamma_i N\right)$$
$$= C_{i,1/2,\mathrm{FA}}^{\Lambda\Lambda}\left(\bar{\Sigma}\Gamma_i\Sigma\right)\left(\bar{N}\Gamma_i N\right). \qquad (12)$$

4) The Lagrangians for the isospin $I=1/2$ $\Lambda N \to \Sigma N$ reaction are:

$$\mathcal{L}_{1/2,\mathrm{FS}}^{\Lambda\Sigma} = \left(\frac{1}{2}C_i^1 - C_i^2\right)\left(\bar{\Lambda}\Gamma_i\Sigma\right)\left(\bar{N}\Gamma_i N\right)$$
$$\equiv C_{i,1/2,\mathrm{FS}}^{\Lambda\Sigma}\left(\bar{\Lambda}\Gamma_i\Sigma\right)\left(\bar{N}\Gamma_i N\right)$$
$$= 3\left(C_{i,1/2,\mathrm{FS}}^{\Lambda\Lambda} - C_{i,1/2,\mathrm{FS}}^{\Sigma\Sigma}\right)\left(\bar{\Lambda}\Gamma_i\Sigma\right)\left(\bar{N}\Gamma_i N\right), \quad (13)$$

$$\mathcal{L}_{1/2,\mathrm{FA}}^{\Lambda\Sigma} = -\left(\frac{3}{2}C_i^1 - C_i^2\right)\left(\bar{\Lambda}\Gamma_i\Sigma\right)\left(\bar{N}\Gamma_i N\right)$$
$$\equiv C_{i,1/2,\mathrm{FA}}^{\Lambda\Sigma}\left(\bar{\Lambda}\Gamma_i\Sigma\right)\left(\bar{N}\Gamma_i N\right). \qquad (14)$$

The superscript YY' denotes the hyperons in the reaction of $YN \to Y'N$. Strict SU(3) symmetry is imposed, as shown in the second line of Eqs. (11-13). Note that the LECs $C_i^{1,2,3}$ here are different from those in Eq. (4) due to the application of Fierz rearrangement [57]. The potentials of the contact terms are derived from Eqs. (7-

14), which can be symbolically written as

$$V_{\mathrm{CT}}^{YY'}=C_i^{YY'}(\bar{u}_3\Gamma_i u_1)(\bar{u}_4\Gamma_i u_2), \qquad (15)$$

where $C_i^{YY'}$ could be $C_{i,1/2,\mathrm{FS}}^{\Lambda\Lambda}$, $C_{i,1/2,\mathrm{FA}}^{\Lambda\Lambda}$, $C_{i,1/2,\mathrm{FS}}^{\Sigma\Sigma}$, $C_{i,1/2,\mathrm{FA}}^{\Sigma\Sigma}$ and $C_{i,1/2,\mathrm{FA}}^{\Lambda\Sigma}$. They are first calculated in the helicity basis and then transformed to the $|LSJ\rangle$ ba-

sis [33]. We found that they contribute to all partial waves that have total angular momentum $J\leq 1$ (except for the $^1P_1-^3P_1$ mixing). We choose the LECs in $^1S_0$, $^3S_1$ and $^3P_1$ to be independent[1], which is consistent with the NN interactions [84]. The partial wave projected potentials are

$$V_{\mathrm{CT}}^{YY'}(^1S_0)=\xi_B\left[(C_1^{YY'}+C_2^{YY'}-6C_3^{YY'}+3C_4^{YY'})(1+R_p^2R_{p'}^2)+(3C_2^{YY'}+6C_3^{YY'}+C_4^{YY'}+C_5^{YY'})(R_p^2+R_{p'}^2)\right]$$
$$\equiv\xi_B\left[C_{1S0}^{YY'}(1+R_p^2R_{p'}^2)+\hat{C}_{1S0}^{YY'}(R_p^2+R_{p'}^2)\right], \qquad (16)$$

$$V_{\mathrm{CT}}^{YY'}(^3S_1)=\xi_B\left[\frac{1}{9}(C_1^{YY'}+C_2^{YY'}+2C_3^{YY'}-C_4^{YY'})(9+R_p^2R_{p'}^2)+\frac{1}{3}(C_2^{YY'}+2C_3^{YY'}-C_4^{YY'}-C_5^{YY'})(R_p^2+R_{p'}^2)\right]$$
$$\equiv\xi_B\left[\frac{1}{9}C_{3S1}^{YY'}(9+R_p^2R_{p'}^2)+\frac{1}{3}\hat{C}_{3S1}^{YY'}(R_p^2+R_{p'}^2)\right], \qquad (17)$$

$$V_{\mathrm{CT}}^{YY'}(^3P_1)=\xi_B\left[-\frac{4}{3}(C_1^{YY'}-2C_2^{YY'}+4C_3^{YY'}+2C_4^{YY'}-C_5^{YY'})R_pR_{p'}\right]\equiv\xi_B\left[-\frac{4}{3}C_{3P1}^{YY'}R_pR_{p'}\right], \qquad (18)$$

$$V_{\mathrm{CT}}^{YY'}(^3P_0)=\xi_B\left[-2(C_1^{YY'}-4C_2^{YY'}-4C_4^{YY'}+C_5^{YY'})R_pR_{p'}\right]=\xi_B\left[-2(-C_{1S0}^{YY'}-\hat{C}_{1S0}^{YY'}+2C_{3S1}^{YY'}-2\hat{C}_{3S1}^{YY'})R_pR_{p'}\right], \qquad (19)$$

$$V_{\mathrm{CT}}^{YY'}(^1P_1)=\xi_B\left[-\frac{2}{3}(C_1^{YY'}+C_5^{YY'})R_pR_{p'}\right]=\xi_B\left[-\frac{2}{3}(C_{3S1}^{YY'}-\hat{C}_{3S1}^{YY'})R_pR_{p'}\right], \qquad (20)$$

$$V_{\mathrm{CT}}^{YY'}(^3S_1-^3D_1)=\xi_B\left[\frac{2}{9}\sqrt{2}(C_1^{YY'}+C_2^{YY'}+2C_3^{YY'}-C_4^{YY'})R_p^2R_{p'}^2+\frac{2}{3}\sqrt{2}(C_2^{YY'}+2C_3^{YY'}-C_4^{YY'}-C_5^{YY'})R_p^2\right]$$
$$=\xi_B\left[\frac{2}{9}\sqrt{2}C_{3S1}^{YY'}R_p^2R_{p'}^2+\frac{2}{3}\sqrt{2}\hat{C}_{3S1}^{YY'}R_p^2\right], \qquad (21)$$

$$V_{\mathrm{CT}}^{YY'}(^3D_1-^3S_1)=\xi_B\left[\frac{2}{9}\sqrt{2}(C_1^{YY'}+C_2^{YY'}+2C_3^{YY'}-C_4^{YY'})R_p^2R_{p'}^2+\frac{2}{3}\sqrt{2}(C_2^{YY'}+2C_3^{YY'}-C_4^{YY'}-C_5^{YY'})R_{p'}^2\right]$$
$$=\xi_B\left[\frac{2}{9}\sqrt{2}C_{3S1}^{YY'}R_p^2R_{p'}^2+\frac{2}{3}\sqrt{2}\hat{C}_{3S1}^{YY'}R_{p'}^2\right], \qquad (22)$$

$$V_{\mathrm{CT}}^{YY'}(^3D_1)=\xi_B\left[\frac{8}{9}(C_1^{YY'}+C_2^{YY'}+2C_3^{YY'}-C_4^{YY'})R_p^2R_{p'}^2\right]=\xi_B\left[\frac{8}{9}C_{3S1}^{YY'}R_p^2R_{p'}^2\right], \qquad (23)$$

where $\xi_B=N_p^2N_{p'}^2$, $R_p=|\boldsymbol{p}|/(E_p+M_B)$, $R_{p'}=|\boldsymbol{p'}|/(E_{p'}+M_B)$ and $M_B=1080$ MeV stands for the SU(3) average mass of the octet baryons in the chiral limit[2]. $\boldsymbol{p}$ and $\boldsymbol{p'}$ denote the initial and final momenta, respectively. Note that the second line of Eq. (19) for $V_{\mathrm{CT}}^{YY'}(^3P_0)$ is only valid for NN interactions, because the structures of the Lagrangians for $^1S_0$ and $^3S_1$ partial waves are different in $\Lambda N-\Sigma N$ systems, as shown in Eqs. (7–14). To recover the potentials in the HB approach we simply take $R_p=R_{p'}=0$ and $\xi_B=1$. The independent potentials respecting SU(3) symmetry are shown in Table 1.

Table 1. Independent contact terms and LECs of strangeness $S=-1$ YN system.

channel	I	V		
		$^1S_0$	$^3P_1$	$^3S_1$
$\Lambda N\to\Lambda N$	$\frac{1}{2}$	$V_{1S0}^{\Lambda\Lambda}$	$V_{3P1}^{\Lambda\Lambda}$	$V_{3S1}^{\Lambda\Lambda}$
$\Lambda N\to\Sigma N$	$\frac{1}{2}$	$3(V_{1S0}^{\Lambda\Lambda}-V_{1S0}^{\Sigma\Sigma})$	$3(V_{3P1}^{\Lambda\Lambda}-V_{3P1}^{\Sigma\Sigma})$	$V_{3S1}^{\Lambda\Sigma}$
$\Sigma N\to\Sigma N$	$\frac{1}{2}$	$9V_{1S0}^{\Lambda\Lambda}-8V_{1S0}^{\Sigma\Sigma}$	$9V_{3P1}^{\Lambda\Lambda}-8V_{3P1}^{\Sigma\Sigma}$	$V_{3S1}^{\Lambda\Lambda}$
$\Sigma N\to\Sigma N$	$\frac{3}{2}$	$V_{1S0}^{\Sigma\Sigma}$	$V_{3P1}^{\Sigma\Sigma}$	$V_{3S1}^{\Sigma\Sigma}$

---

1) The other choice is to take those in $^1S_0$, $^3S_1$ and $^3P_0$ partial waves.

2) The baryon mass difference is treated as a higher order correction in chiral perturbation theory.

The analytical form of the potentials, e.g., $V_{1S0}^{\Lambda\Lambda}$, $V_{1P1}^{\Lambda\Lambda}$, can be obtained from Eqs. (16–23). Finally we have 12 independent LECs: $C_{1S0}^{\Lambda\Lambda}$, $\hat{C}_{1S0}^{\Lambda\Lambda}$, $C_{1S0}^{\Sigma\Sigma}$, $\hat{C}_{1S0}^{\Sigma\Sigma}$, $C_{3S1}^{\Lambda\Lambda}$, $\hat{C}_{3S1}^{\Lambda\Lambda}$, $C_{3S1}^{\Sigma\Sigma}$, $\hat{C}_{3S1}^{\Sigma\Sigma}$, $C_{3S1}^{\Lambda\Sigma}$, $\hat{C}_{3S1}^{\Lambda\Sigma}$, $C_{3P1}^{\Lambda\Lambda}$, $C_{3P1}^{\Sigma\Sigma}$. The other three LECs only contribute to the strangeness $S=-2$ system.

2.2.2 One-pseudoscalar-meson-exchange potentials

At LO, we have seven Feynman diagrams for strangeness $S=-1$ systems, as shown in Fig. 3. The one-pseudoscalar-meson-exchange potentials are derived from the covariant SU(3) meson-baryon Lagrangian,

$$\mathcal{L}_{MB}^{(1)}=\mathrm{tr}\left(\bar{B}\left(i\gamma_\mu D^\mu-M_B\right)B-\frac{D}{2}\bar{B}\gamma^\mu\gamma_5\{u_\mu,B\}\right.$$
$$\left.-\frac{F}{2}\bar{B}\gamma^\mu\gamma_5[u_\mu,B]\right), \tag{24}$$

where $D^\mu B=\partial_\mu B+[\Gamma_\mu,B]$ and D and F are the axial vector couplings. In the numerical analysis, we use $D+F=g_A=1.277$ [88] and $F/(F+D)=0.4$, where g_A is the nucleon axial vector coupling constant. Γ_μ and u_μ are the vector and axial vector combinations of the pseudoscalar-meson fields and their derivatives,

$$\Gamma_\mu=\frac{1}{2}\left(u^\dagger\partial_\mu u+u\partial_\mu u^\dagger\right), \quad u_\mu=i(u^\dagger\partial_\mu u-u\partial_\mu u^\dagger),$$

where $u^2=U=\exp\left(i\frac{\sqrt{2}\phi}{f_0}\right)$, with the pseudoscalar-meson decay constant $f_0\simeq f_\pi=92.2$ MeV [88], and the traceless matrix ϕ collecting the pseudoscalar-meson fields is:

$$\phi=\begin{pmatrix} \frac{\pi^0}{\sqrt{2}}+\frac{\eta}{\sqrt{6}} & \pi^+ & K^+ \\ \pi^- & -\frac{\pi^0}{\sqrt{2}}+\frac{\eta}{\sqrt{6}} & K^0 \\ K^- & \bar{K}^0 & -\frac{2\eta}{\sqrt{6}} \end{pmatrix}. \tag{25}$$

The potentials for OPME can be expressed in a generic form:

$$V_{\mathrm{OPME}} = -N_{B_1B_3\phi}N_{B_2B_4\phi}\frac{(\bar{u}_3\gamma^\mu\gamma_5 q_\mu u_1)(\bar{u}_4\gamma^\nu\gamma_5 q_\nu u_2)}{q^2-m^2}$$
$$\times\mathcal{I}_{B_1B_2\to B_3B_4}, \tag{26}$$

where $q=p'-p$ is the momentum transfer, $q^2=(E_{p'}-E_p)^2-(\boldsymbol{p}'-\boldsymbol{p})^2$, and m is the mass of the exchanged pseudoscalar meson. The SU(3) coefficient $N_{BB'\phi}$ and isospin factor $\mathcal{I}_{B_1B_2\to B_3B_4}$ are listed in Refs. [57, 74]. The retardation effects are included in the denominator. Just like the contact terms, Eqs. (15–23), the average baryon mass $M_B=1080$ MeV is used in the baryon spinors $u(\bar{u})$ and energies $E_{p(p')}$. One can easily obtain V_{OPME} in the $|LSJ\rangle$ basis following the same procedure as that for the contact terms. We note that by the mass differences of the exchanged mesons[1] the SU(3) symmetry is broken.

In our covariant power counting scheme we keep the complete form of the Dirac spinors and do not perform expansions in terms of small external three momenta, different from what done in the HB approach. In relativistic atomic and nuclear structure studies, the small components of the Dirac spinors have been shown to play an important role, mostly of a dynamical nature. As we will see below, they also play an important role in the present study and result in a good description of YN scattering data. Because the small components are retained, once written in terms of three-momenta and Pauli matrices, the relativistic potential contains terms of higher chiral order in the HB language, similar to the one-baryon sector in covariant chiral perturbation theory. Furthermore, we can see that the LO potentials obtained in the EG approach are the same as those of the HB approach [74], different from the relativistic potentials.
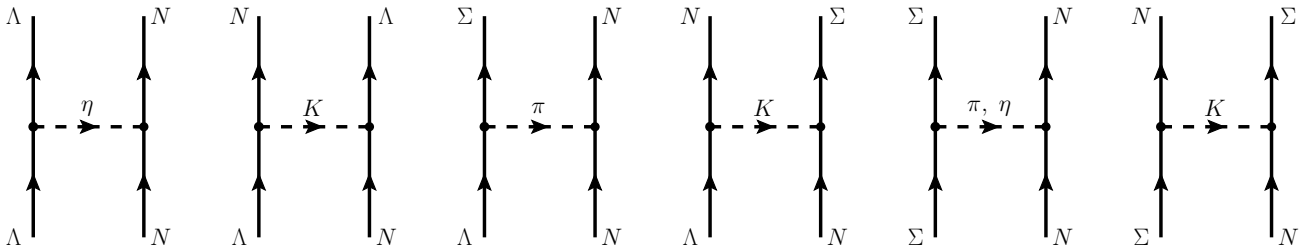

Fig. 3.   The one-pseudoscalar-meson exchange diagrams in the $\Lambda N-\Sigma N$ system.

2.3 Scattering equation

The infrared enhancement in two-baryon propagations gives the theoretical argument for low-energy baryon-baryon interactions to be non-perturbative [55]. As a result, one needs to iterate the potentials in the Bethe-Salpeter equation. In practice this is difficult. A three-dimensional reduction of the Bethe-Salpeter equation is often used [89]. In the present work, following Ref. [74], we use the coupled-channel Kadyshevsky equation

1) We have used $m_\pi=138.039$ MeV, $m_K=495.645$ MeV and $m_\eta=547.853$ MeV in the numerical calculations.

$$T_{\rho\rho'}^{\nu\nu',J}(\boldsymbol{p'},\boldsymbol{p};\sqrt{s})=V_{\rho\rho'}^{\nu\nu',J}(\boldsymbol{p'},\boldsymbol{p})+\sum_{\rho'',\nu''}\int_0^\infty\frac{\mathrm{d}p''p''^2}{(2\pi)^3}\frac{M_{B_{1,\nu''}}M_{B_{2,\nu''}}\,V_{\rho\rho''}^{\nu\nu'',J}(\boldsymbol{p'},\boldsymbol{p''})\,T_{\rho''\rho'}^{\nu''\nu',J}(\boldsymbol{p''},\boldsymbol{p};\sqrt{s})}{E_{1,\nu''}E_{2,\nu''}(\sqrt{s}-E_{1,\nu''}-E_{2,\nu''}+i\epsilon)},\tag{27}$$

where $\sqrt{s}$ is the total energy of the baryon-baryon system in the center-of-mass frame and $E_{n,\nu''}=\sqrt{\boldsymbol{p''}+M_{B_{n,\nu''}}}$, $(n=1,2)$. The labels ν,ν',ν'' denote the particle channels, and ρ,ρ',ρ'' denote the partial waves. Relativistic kinematics is used throughout to relate the laboratory momenta to the center-of-mass momenta.

To regularize the integration in the high-momentum region, baryon-baryon potentials are multiplied with an exponential form factor,

$$f_{\Lambda_F}(\boldsymbol{p},\boldsymbol{p'})=\exp\left[-\left(\frac{\boldsymbol{p}}{\Lambda_F}\right)^{2n}-\left(\frac{\boldsymbol{p'}}{\Lambda_F}\right)^{2n}\right],\tag{28}$$

where $n=2$ [90]. Note that Eq. (28) is not a covariant cutoff function. Although there exist covariant cutoff functions of q^2, they are not favored in constructing chiral forces because they will introduce additional angular dependence to partial wave potentials and thus affect the interpretation of contact interactions. It would be interesting to construct a separable and covariant cutoff function and study its consequences in the future.

The Kadyshevsky equation is solved in the particle basis in order to properly account for the physical thresholds and the Coulomb force in charged channels. The latter is treated with the Vincent-Phatak method [91].

3　Fitting procedure

In our approach, there are 12 LECs that need to be pinned down by fitting to the 36 YN scattering data points as done in Ref. [74], which consist of 35 cross sections [92–95] and a Σ^-p inelastic capture ratio at rest [98].

Due to the poor quality of experimental data, it is customary to consider the hypertriton $^3_\Lambda$H binding energy [99, 100] as a further constraint, which is crucial in fixing the relative strength of the $^1S_0$ and $^3S_1$ contributions to Λp scattering. However, we are unable to perform a 3-body calculation at present, so we use as benchmarks the Λp S-wave scattering lengths extracted in the LO [57] and next-to-leading order (NLO) [59] HB calculations, mainly because they combine to describe the hypertriton very well [101]. In addition, it seems necessary that $a_{1S0}^{\Lambda p}$ should be neither smaller nor too much larger than $a_{3S1}^{\Lambda p}$, as shown in Ref. [102].

Another constraint that should be considered is the Σ^+p $^3S_1$ scattering length. A repulsive ΣN interaction with isospin $I=3/2$ is obtained from recent experi-

ments [103–109]. In addition, the conventional G-matrix calculations [110] indicate that the $^3S_1$ partial wave for $I=3/2$ ΣN should be at least moderately repulsive, therefore in our fits we require a positive $a_{3S1}^{\Sigma^+p}$.

Previous works in χEFT [57, 59, 74] showed that the optimum cutoff Λ_F may be around 600 MeV. Therefore we first tentatively fix Λ_F at 600 MeV. With this cutoff we find that the best description of the experimental data yields $a_{3S1}^{\Lambda p}\approx-1.30\pm0.02$ fm and $a_{1S0}^{\Lambda p}\approx-2.44^{+0.16}_{-0.54}$ fm. These numbers are between the LO and NLO HB results, which are $a_{3S1}^{\Lambda p}=-1.23$ fm (LO), $a_{3S1}^{\Lambda p}=-1.54$ fm (NLO), $a_{1S0}^{\Lambda p}=-1.91$ fm (LO), and $a_{1S0}^{\Lambda p}=-2.91$ fm (NLO). Best fits within $\Lambda_F=500$–850 MeV yield similar scattering lengths. In the results presented below, we fix $a_{3S1}^{\Lambda p}=-1.32$ fm and $a_{1S0}^{\Lambda p}=-2.44$ fm[1]). It should be noted that at present we could in principle choose other combinations within the uncertainties allowed in the best fits. To fix them uniquely, more experimental inputs are needed.

We have made an attempt at a combined fit to the NN and YN data, in which strict SU(3) symmetry was imposed upon the contact terms so that no additional LECs are needed. However, we failed to describe the NN and YN data simultaneously. As a result, consistent with previous NLO results in the HB approach [59], we conclude that one needs to treat SU(3) symmetry breaking more carefully in order to simultaneously describe both the NN and the YN systems in χEFT.

4　Results and discussion

With the three additional constraints $a_{1S0}^{\Lambda p}=-2.44$ fm, $a_{3S1}^{\Lambda p}=-1.32$ fm and $a_{3S1}^{\Sigma^+p}>0$ as explained above, we perform a fit to the 36 scattering data points while varying the cutoff Λ_F. The dependence of χ^2 on the cutoff is shown in Fig. 4, in comparison with other approaches. One can see that our new covariant χEFT approach shows a clear improvement in describing the YN data compared with the HB and EG approach at LO, and the cutoff dependence is much mitigated, both of which are comparable with the NLO HB approach [59].

The minimum value of the χ^2 is about 16.1, located at $\Lambda_F=550$–650 MeV. Note that the NSC97a-f [30] models, which provide the best description among the phenomenological potentials of the 36 scattering data points, also have a χ^2 around 16.

The best fitted LECs obtained with $\Lambda_F=600$ MeV are listed in Table 2. Since the LECs in the Λp $^1S_0$ par-

---

1) We have chosen a larger $a_{3S1}^{\Lambda p}$ given the fact that most phenomenological studies seem to prefer a larger scattering length in this channel.

tial wave cannot be uniquely determined, as mentioned previously, we only show a typical case here. One should note that these LECs are certain combinations of those appearing in the Lagrangians, and hence they are not necessarily of the same order of magnitude (see, e.g., Refs. [57, 59]).
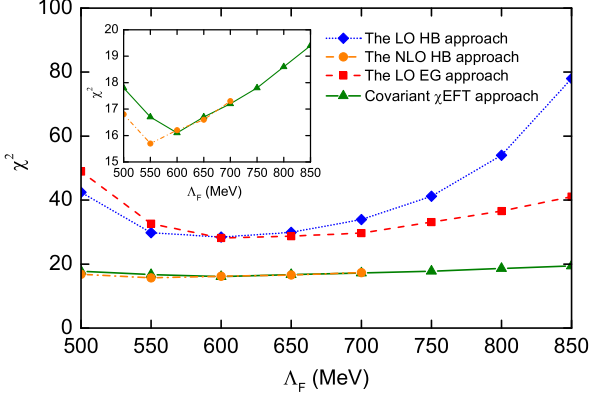

Fig. 4. (color online) χ^2 as a function of the cutoff in the covariant χEFT approach at LO (green solid line), the HB approach at LO (blue dotted line), NLO (orange dashed-dotted line) [59] and the EG approach at LO (red dashed line).

In Fig. 5 we compare the descriptions of the experimental cross sections that we have used in the fitting procedure with the LO HB approach. The NSC97f [30] and Jülich 04 results [35] are also shown for comparison. It is clear that the covariant χEFT approach can reproduce the experimental data rather well. The cusp at the ΣN threshold in the $\Lambda p \to \Lambda p$ reaction is also reproduced well. Note that the experimental data with $P_{\text{lab}} > 300$ MeV are not used in the fitting procedure.

Due to the lack of near-threshold experimental data, the value of the $\Lambda p \to \Lambda p$ cross section at rest is not yet known. Our value is about 350 mb, which is smaller than the two phenomenological models. Our result in the $\Sigma^- p \to \Lambda n$ reaction is similar to the LO HB approach and NSC97f results, but quite different from the Jülich 04 model. This channel can partially reflect the nature of $\Lambda N - \Sigma N$ coupling, which is crucial in hypernuclear structure calculations [19]. It is interesting to note that the Jülich 04 model predicts an overbound Λ single particle potential $U_\Lambda(0)$ in G-matrix calculations. On the other hand, the results from the former two are much closer to the empirical value, c.f. Ref. [110] and references therein. In addition, the differential cross sections shown in Fig. 6 are also well predicted within experimental uncertainties, although those data are not taken into account in the fitting procedure.

Table 2.   Low-energy constants (in units of 10^4 GeV^{-2}) at $\Lambda_F = 600$ MeV in the covariant χEFT approach.

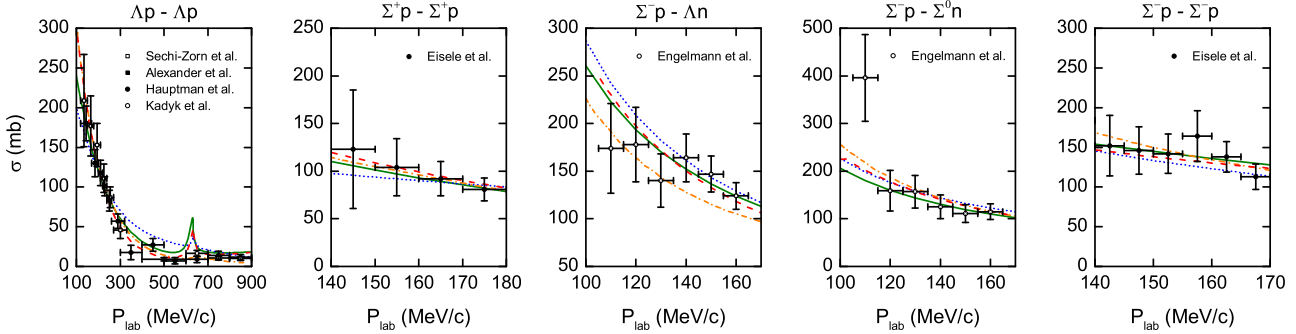| LECs	$C_{1S0}^{\Lambda\Lambda}$	$C_{1S0}^{\Sigma\Sigma}$	$C_{3S1}^{\Lambda\Lambda}$	$C_{3S1}^{\Sigma\Sigma}$	$C_{3S1}^{\Lambda\Sigma}$	$\hat{C}_{1S0}^{\Lambda\Lambda}$	$\hat{C}_{1S0}^{\Sigma\Sigma}$	$\hat{C}_{3S1}^{\Lambda\Lambda}$	$\hat{C}_{3S1}^{\Sigma\Sigma}$	$\hat{C}_{3S1}^{\Lambda\Sigma}$	$C_{3P1}^{\Lambda\Lambda}$	$C_{3P1}^{\Sigma\Sigma}$
	-0.0096	-0.0276	0.0110	0.0872	0.0257	4.2463	4.6182	0.3660	-0.4132	0.8499	0.2044	0.2616

Fig. 5. (color online) Cross sections in the covariant χEFT approach (green solid lines) and HB approach (blue dotted lines) at LO as functions of the laboratory momentum at $\Lambda_F = 600$ MeV. For reference, the NSC97f [30] (red dashed lines) and Jülich 04 [35] (orange dashed-dotted lines) results are also shown. The experimental data are taken from Sechi-Zorn et al. [92], Alexander et al. [93], Eisele et al. [94], Engelmann et al. [95], Hauptman et al. [96] and Kadyk et al. [97].
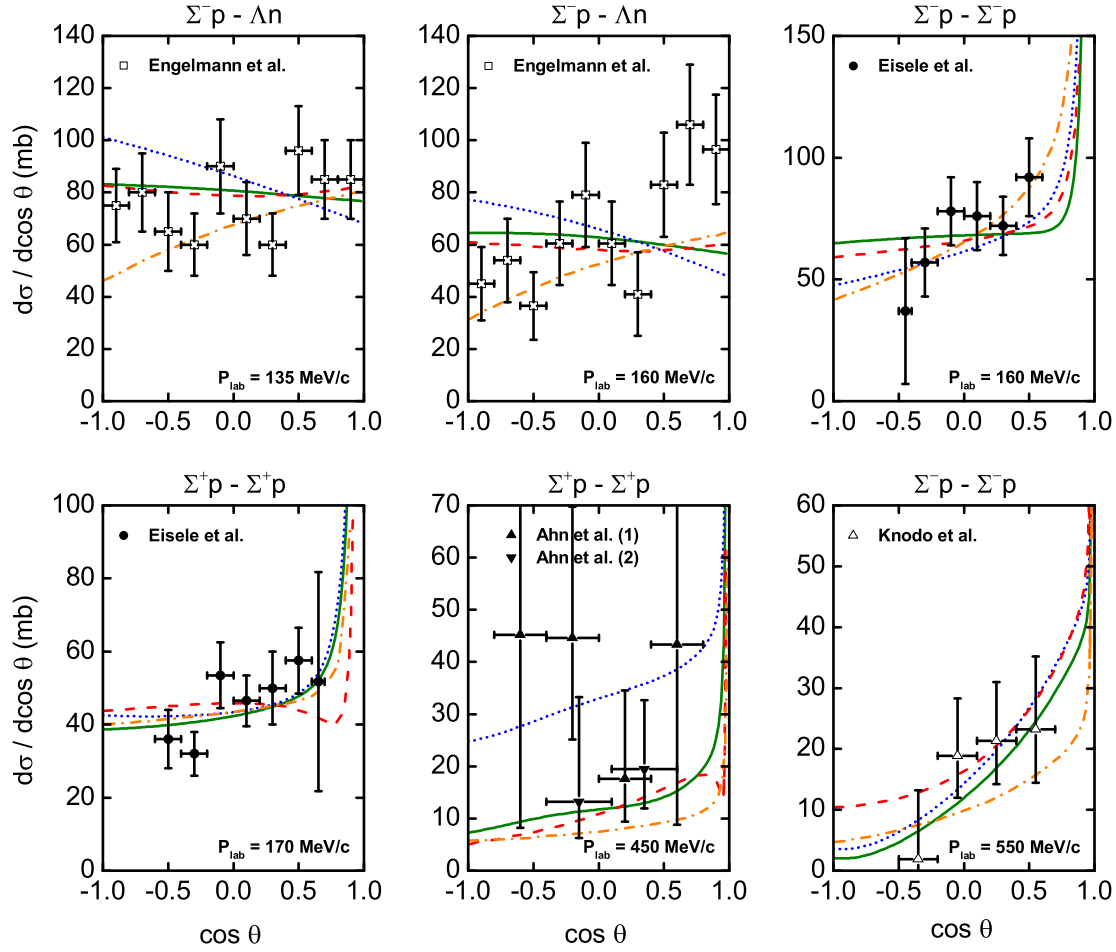
Fig. 6.   (color online) Differential cross sections as a function of $\cos\theta$ at various laboratory momenta P_{lab}, where θ is the center-of-mass scattering angle. The covariant χEFT approach is shown by the green solid lines, the HB approach at LO by the blue dotted lines, the NSC97f [30] results by the red dashed lines, and the Jülich 04 [35] results by the orange dashed-dotted lines. The experimental data are taken from Engelmann et al. [95], Eisele et al. [94], Ahn et al. [111, 112] and Kohno et al. [113].

S- and P-wave phase shifts of Λp and $\Sigma^+ p$ reactions are shown in Figs. 7, 8. The $^1S_0$ and $^3P_0$ phase shifts are quite different from those of the LO HB approach, but the $^3P_2$ phase shifts are similar, where only OPME terms contribute. Furthermore, the $^1S_0$ phase shifts are similar to those of the NLO HB approach [59].

The improved description of the scattering data by the covariant χEFT scheme for the most part arises from the contact terms. In the LO HB approach, contact terms only appear in central and spin-spin potentials without momentum dependence, which only con-

tribute to the $^1S_0$ and $^3S_1$ partial waves. In covariant power counting, tensor, spin-orbit and quadratic spin-orbit terms appear at LO in addition to the central and spin-spin terms, namely the momentum dependent terms of $R^2_{p\ (p')}$ in Eqs. (16-23). These terms are responsible for the improved description. On the other hand, relativistic corrections to the OPME terms are small. As a result, phase shifts of higher partial waves where only such terms contribute are similar in the covariant and HB approaches at LO. A related discussion for the NN sector can be found in Ref. [84].
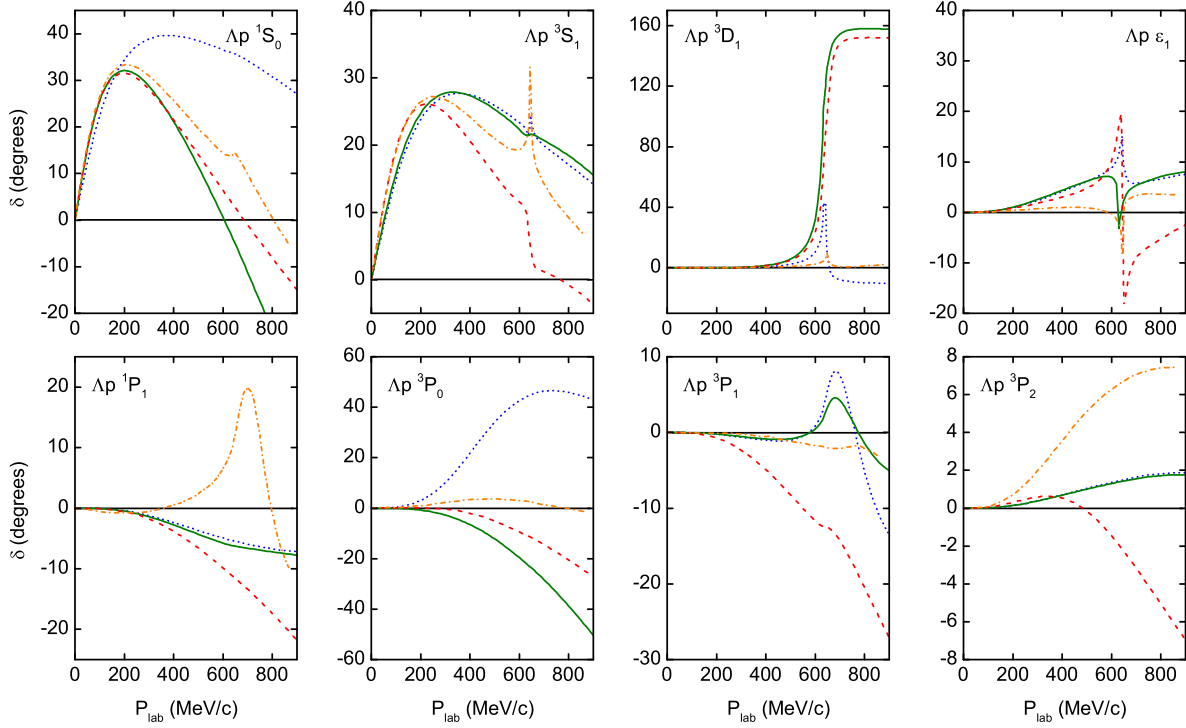
Fig. 7.   (color online) Λp S- and P-wave phase shifts in the covariant χEFT approach (green solid lines) and HB approach (blue dotted lines) at LO as functions of the laboratory momentum at $\Lambda_F = 600$ MeV. For reference, the NSC97f [30] (red dashed lines) and Jülich 04 [35] (orange dashed-dotted lines) results are also shown.
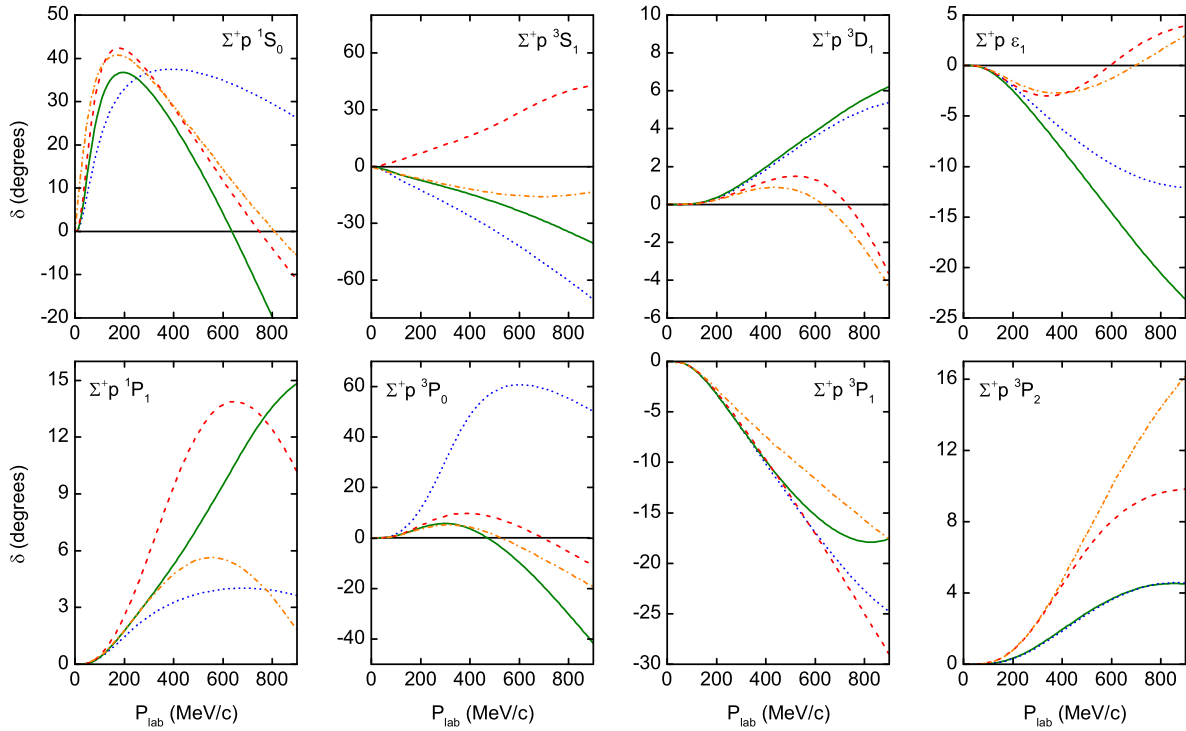

Fig. 8.   (color online) $\Sigma^+ p$ S- and P-wave phase shifts in the covariant χEFT approach (green solid lines) and HB approach (blue dotted lines) at LO as functions of the laboratory momentum at $\Lambda_F = 600$ MeV. For reference, the NSC97f [30] (red dashed lines) and Jülich 04 [35] (orange dashed-dotted lines) results are also shown.

5   Summary and outlook

We have studied strangeness $S=-1$ hyperon-nucleon scattering at leading order in a covariant framework of chiral effective field theory. Starting from the covariant chiral Lagrangian, the small components of the baryon spinors are retained in deriving the potentials in order to preserve Lorentz invariance. Strict SU(3) symmetry is imposed on the contact terms, which yield 12 independent low energy constants. SU(3) symmetry is broken in the one-pseudoscalar-meson-exchange potentials because of the mass difference of exchanged mesons.

The potentials are iterated using the Kadyshevsky equation. A quite satisfactory description of the 36 hyperon-nucleon scattering data points is obtained and the cut-off dependence is shown to be mitigated, both of which are comparable with the next-to-leading order heavy baryon approach. However, one cannot achieve a simultaneous description of the nucleon-nucleon phase shifts and strangeness $S=-1$ hyperon-nucleon scattering data at leading order. The relativistic interactions obtained in the this work may provide essential inputs to relativistic hypernuclear structure studies, e.g., relativistic Brueckner-Hartree-Fork theory in many-body systems.

References

1 M. Gell-Mann, Phys. Rev., **92**: 833 (1953)
2 T. Nakano and K. Nishijima, Prog. Theor. Phys., **10**: 581 (1953)
3 M. Danysz, and J. Pniewski, Philos. Mag. Ser. 5, **44**: 348 (1953)
4 M. Bedjidian et al (CERN-Lyon-Warsaw Collaboration), Phys. Lett. B, **83**: 252 (1979)
5 R. L. Jaffe, Phys. Rev. Lett., **38**: 195 (1977) Erratum: [Phys. Rev. Lett., **38**: 617 (1977)]
6 A. Nogga, H. Kamada, and W. Glöckle, Phys. Rev. Lett., **88**: 172501 (2002) [nucl-th/0112060]
7 D. Gazda and A. Gal, Phys. Rev. Lett., **116**: 122501 (2016) [arXiv:1512.01049 [nucl-th]]
8 S. R. Beane et al (NPLQCD Collaboration), Phys. Rev. Lett., **106**: 162001 (2011) [arXiv:1012.3812 [hep-lat]]
9 T. Inoue et al (HAL QCD Collaboration), Phys. Rev. Lett., **106**: 162002 (2011) [arXiv:1012.5928 [hep-lat]]
10 J. Haidenbauer and U. -G. Meißner, Phys. Lett. B, **706**: 100 (2011) [arXiv:1109.3590 [hep-ph]]
11 Y. Yamaguchi and T. Hyodo, arXiv:1607.04053 [hep-ph]
12 T. Gogami et al, Phys. Rev. C, **93**(3): 034314 (2016) [arXiv:1511.04801 [nucl-ex]]
13 A. Esser et al (A1 Collaboration), Phys. Rev. Lett., **114**(23): 232501 (2015) [arXiv:1501.06823 [nucl-ex]]
14 T. O. Yamamoto et al (J-PARC E13 Collaboration), Phys. Rev. Lett., **115**: 222501 (2015) [arXiv:1508.00376 [nucl-ex]]
15 J. K. Ahn et al (E373 (KEK-PS) Collaboration), Phys. Rev. C, **88**: 014003 (2013)
16 K. Nakazawa et al, PTEP, **2015**(3): 033D02 (2015)
17 See list of proposals at http://j-parc.jp/researcher/Hadron/en/Proposal_e.html
18 F. Hauenstein et al (COSY-TOF Collaboration), arXiv:1607.04783 [nucl-ex]
19 E. Hiyama, S. Ohnishi, B. F. Gibson, and T. A. Rijken, Phys. Rev. C, **89**: 061302 (2014) [arXiv:1405.2365 [nucl-th]]
20 X. R. Zhou, H.-J. Schulze, H. Sagawa, C. X. Wu, and E. G. Zhao, Phys. Rev. C, **76**: 034312 (2007)
21 E. Massot, J. Margueron, and G. Chanfray, Europhys. Lett., **97**: 39002 (2012) [arXiv:1201.2772 [nucl-th]]
22 H.-J. Schulze and T. Rijken, Phys. Rev. C, **84**: 035801 (2011)
23 J. N. Hu, A. Li, H. Toki, and W. Zuo, Phys. Rev. C, **89**: 025802 (2014) [arXiv:1307.4154 [nucl-th]]
24 T. Miyatsu, S. Yamamuro, and K. Nakazato, Astrophys. J., **777**: 4 (2013) [arXiv:1308.6121 [astro-ph.HE]]
25 R. Mallick, Phys. Rev. C, **87**: 025804 (2013) [arXiv:1207.4872 [astro-ph.HE]]
26 P. Demorest, T. Pennucci, S. Ransom, M. Roberts, and J. Hessels, Nature, **467**: 1081 (2010) [arXiv:1010.5788 [astro-ph.HE]]
27 J. Antoniadis et al, Science, **340**: 6131 (2013) [arXiv:1304.6875 [astro-ph.HE]]
28 M. M. Nagels, T. A. Rijken, and J. J. de Swart, Phys. Rev. D, **15**: 2547 (1977)
29 P. M. M. Maessen, T. A. Rijken, and J. J. de Swart, Phys. Rev. C, **40**: 2226 (1989)
30 T. A. Rijken, V. G. J. Stoks, and Y. Yamamoto, Phys. Rev. C, **59**: 21 (1999) [nucl-th/9807082]
31 T. A. Rijken and Y. Yamamoto, Phys. Rev. C, **73**: 044008 (2006) [nucl-th/0603042]
32 M. M. Nagels, T. A. Rijken, and Y. Yamamoto, arXiv:1501.06636 [nucl-th]
33 B. Holzenkamp, K. Holinde, and J. Speth, Nucl. Phys. A, **500**: 485 (1989)
34 A. Reuber, K. Holinde, and J. Speth, Nucl. Phys. A, **570**: 543 (1994)
35 J. Haidenbauer and U. -G. Meißner, Phys. Rev. C, **72**: 044005 (2005) [nucl-th/0506019]
36 U. Straub, Z. Y. Zhang, K. Brauer, A. Faessler, S. B. Khadkikar, and G. Lubeck, Nucl. Phys. A, **483**: 686 (1988)
37 U. Straub, Z. Y. Zhang, K. Braeuer, A. Faessler, S. B. Khadkikar, and G. Luebeck, Nucl. Phys. A, **508**: 385C (1990)
38 Z. Y. Zhang, A. Faessler, U. Straub, and L. Y. Glozman, Nucl. Phys. A, **578**: 573 (1994)
39 Z. Y. Zhang, Y. W. Yu, P. N. Shen, L. R. Dai, A. Faessler, and U. Straub, Nucl. Phys. A, **625**: 59 (1997)
40 J. L. Ping, F. Wang, and J. T. Goldman, Nucl. Phys. A, **657**: 95 (1999) [nucl-th/9812068]
41 Y. Fujiwara, C. Nakamoto, and Y. Suzuki, Phys. Rev. Lett., **76**: 2242 (1996)
42 Y. Fujiwara, Y. Suzuki, and C. Nakamoto, Prog. Part. Nucl. Phys., **58**: 439 (2007) [nucl-th/0607013]
43 S. R. Beane et al (NPLQCD Collaboration), Nucl. Phys. A, **794**: 62 (2007) [hep-lat/0612026]
44 H. Nemura, N. Ishii, S. Aoki, and T. Hatsuda, Phys. Lett. B, **673**: 136 (2009) [arXiv:0806.1094 [nucl-th]]
45 S. R. Beane et al (NPLQCD Collaboration), Phys. Rev. D, **81**: 054505 (2010) [arXiv:0912.4243 [hep-lat]]
46 T. Inoue et al (HAL QCD Collaboration), Prog. Theor. Phys., **124**: 591 (2010) [arXiv:1007.3559 [hep-lat]]
47 S. R. Beane et al (NPLQCD Collaboration), Phys. Rev. D, **85**: 054511 (2012) [arXiv:1109.2889 [hep-lat]]
48 K. Sasaki et al (HAL QCD Collaboration), PTEP, **2015**: 113B01 (2015) [arXiv:1504.01717 [hep-lat]]
49 T. Doi et al, arXiv:1512.01610 [hep-lat]
50 T. Doi et al, arXiv:1512.04199 [hep-lat]
51 P. F. Bedaque and U. van Kolck, Ann. Rev. Nucl. Part. Sci., **52**: 339 (2002) [nucl-th/0203055]
52 E. Epelbaum, H. W. Hammer, and U. -G. Meißner, Rev. Mod. Phys., **81**: 1773 (2009) [arXiv:0811.1338 [nucl-th]]

53 R. Machleidt and D. R. Entem, Phys. Rept., **503**: 1 (2011) [arXiv:1105.2919 [nucl-th]]
54 S. Weinberg, Phys. Lett. B, **251**: 288 (1990)
55 S. Weinberg, Nucl. Phys. B, **363**: 3 (1991)
56 X. W. Kang, J. Haidenbauer, and U. -G. Meißner, JHEP, **1402**: 113 (2014) [arXiv:1311.1658 [hep-ph]]
57 H. Polinder, J. Haidenbauer, and U. -G. Meißner, Nucl. Phys. A, **779**: 244 (2006) [nucl-th/0605050]
58 J. Haidenbauer, U. -G. Meißner, A. Nogga, and H. Polinder, Lect. Notes Phys., **724**: 113 (2007) [nucl-th/0702015 [NUCL-TH]]
59 J. Haidenbauer, S. Petschauer, N. Kaiser, U.-G. Meißner, A. Nogga, and W. Weise, Nucl. Phys. A, **915**: 24 (2013) [arXiv:1304.5339 [nucl-th]]
60 H. Polinder, J. Haidenbauer, and U.-G. Meißner, Phys. Lett. B, **653**: 29 (2007) [arXiv:0705.3753 [nucl-th]]
61 J. Haidenbauer and U.-G. Meißner, Phys. Lett. B, **684**: 275 (2010) [arXiv:0907.1395 [nucl-th]]
62 J. Haidenbauer, U.-G. Meißner, and S. Petschauer, Nucl. Phys. A, **954**: 273 (2016) [arXiv:1511.05859 [nucl-th]]
63 G. P. Lepage, nucl-th/9706029
64 M. C. Birse, Phys. Rev. C, **74**: 014003 (2006) [nucl-th/0507077]
65 A. Nogga, R. G. E. Timmermans, and U. van Kolck, Phys. Rev. C, **72**: 054006 (2005) [nucl-th/0506005]
66 E. Epelbaum and U.-G. Meißner, Few Body Syst., **54**: 2175 (2013) [nucl-th/0609037]
67 B. Long and U. van Kolck, Annals Phys., **323**: 1304 (2008) [arXiv:0707.4325 [quant-ph]]
68 C.-J. Yang, C. Elster, and D. R. Phillips, Phys. Rev. C, **80**: 044002 (2009) [arXiv:0905.4943 [nucl-th]]
69 M. P. Valderrama, Phys. Rev. C, **83**: 024003 (2011) [arXiv:0912.0699 [nucl-th]]
70 B. Long and C. J. Yang, Phys. Rev. C, **85**: 034002 (2012) [arXiv:1111.3993 [nucl-th]]
71 E. Epelbaum and J. Gegelia, Phys. Lett. B, **716**: 338 (2012) [arXiv:1207.2420 [nucl-th]]
72 E. Epelbaum, A. M. Gasparyan, J. Gegelia, and H. Krebs, Eur. Phys. J. A, **51**: 71 (2015) [arXiv:1501.01191 [nucl-th]]
73 V. G. J. Stoks, R. A. M. Klomp, M. C. M. Rentmeester, and J. J. de Swart, Phys. Rev. C, **48**: 792 (1993)
74 K. -W. Li, X. -L. Ren, L. S. Geng, and B. Long, Phys. Rev. D, **94**: 014029 (2016) [arXiv:1603.07802 [hep-ph]]
75 L. S. Geng, J. Martin Camalich, L. Alvarez-Ruso, and M. J. Vicente Vacas, Phys. Rev. Lett., **101**: 222002 (2008) [arXiv:0805.1419 [hep-ph]]
76 L. S. Geng, J. Martin Camalich, and M. J. Vicente Vacas, Phys. Rev. D, **79**: 094022 (2009) [arXiv:0903.4869 [hep-ph]]
77 L. S. Geng, X. -L. Ren, J. Martin-Camalich, and W. Weise, Phys. Rev. D, **84**: 074024 (2011) [arXiv:1108.2231 [hep-ph]]
78 X. -L. Ren, L. S. Geng, J. Martin Camalich, J. Meng, and H. Toki, JHEP, **1212**: 073 (2012) [arXiv:1209.3641 [nucl-th]]
79 X. -L. Ren, L. -S. Geng, and J. Meng, Phys. Rev. D, **91**: 051502 (2015) [arXiv:1404.4799 [hep-ph]]
80 L. S. Geng, N. Kaiser, J. Martin-Camalich, and W. Weise, Phys. Rev. D, **82**: 054022 (2010) [arXiv:1008.0383 [hep-ph]]
81 L. S. Geng, M. Altenbuchinger, and W. Weise, Phys. Lett. B, **696**: 390 (2011) [arXiv:1012.0666 [hep-ph]]
82 M. Altenbuchinger, L. S. Geng, and W. Weise, Phys. Lett. B,

713: 453 (2012) [arXiv:1109.0460 [hep-ph]]
83 L. S. Geng, Front. Phys., (Beijing) **8**: 328 (2013) [arXiv:1301.6815 [nucl-th]]
84 X. -L. Ren, K. -W. Li, L. S. Geng, B. -W. Long, P. Ring, and J. Meng, arXiv:1611.08475 [nucl-th]
85 L. Girlanda, S. Pastore, R. Schiavilla, and M. Viviani, Phys. Rev. C, **81**: 034005 (2010) [arXiv:1001.3676 [nucl-th]]
86 D. Djukanovic, J. Gegelia, S. Scherer, and M. R. Schindler, Few Body Syst., **41**: 141 (2007) [nucl-th/0609055]
87 S. Petschauer and N. Kaiser, Nucl. Phys. A, **916**: 1 (2013) [arXiv:1305.3427 [nucl-th]]
88 C. Patrignani et al (Particle Data Group), Chin. Phys. C, **40**(10): 100001 (2016)
89 R. M. Woloshyn and A. D. Jackson, Nucl. Phys. B, **64**: 269 (1973)
90 E. Epelbaum, W. Glöckle, and U.-G. Meißner, Nucl. Phys. A, **747**: 362 (2005) [nucl-th/0405048]
91 C. M. Vincent and S. C. Phatak, Phys. Rev. C, **10**: 391 (1974)
92 B. Sechi-Zorn, B. Kehoe, J. Twitty, and R. A. Burnstein, Phys. Rev., **175**: 1735 (1968)
93 G. Alexander, U. Karshon, A. Shapira, G. Yekutieli, R. Engelmann, H. Filthuth, and W. Lughofer, Phys. Rev., **173**: 1452 (1968)
94 F. Eisele, H. Filthuth, W. Foehlisch, V. Hepp, and G. Zech, Phys. Lett. B, **37**: 204 (1971)
95 R. Engelmann, H. Filthuth, V. Hepp, and E. Kluge, Phys. Lett., **21**: 587 (1966)
96 J. M. Hauptman, J. A. Kadyk, and G. H. Trilling, Nucl. Phys. B, **125**: 29 (1977)
97 J. A. Kadyk, G. Alexander, J. H. Chan, P. Gaposchkin, and G. H. Trilling, Nucl. Phys. B, **27**: 13 (1971)
98 V. Hepp and H. Schleich, Z. Phys., **214**: 71 (1968)
99 M. Juric et al, Nucl. Phys. B, **52**: 1 (1973)
100 D. H. Davis, AIP Conf. Proc., **224**: 38 (1991)
101 A. Nogga, Nucl. Phys. A, **914**: 140 (2013)
102 K. Tominaga, T. Ueda, M. Yamaguchi, N. Kijima, D. Okamoto, K. Miyagawa, and T. Yamada, Nucl. Phys. A, **642**: 483 (1998)
103 C. J. Batty, E. Friedman, and A. Gal, Phys. Lett. B, **335**: 273 (1994)
104 J. Mares, E. Friedman, A. Gal, and B. K. Jennings, Nucl. Phys. A, **594**: 311 (1995) [nucl-th/9505003]
105 S. Bart et al, Phys. Rev. Lett., **83**: 5238 (1999)
106 H. Noumi et al, Phys. Rev. Lett., **89**: 072301 (2002) Erratum: [Phys. Rev. Lett., **90**: 049902 (2003)]
107 P. K. Saha et al, Phys. Rev. C, **70**: 044613 (2004) [nucl-ex/0405031]
108 M. Kohno, Y. Fujiwara, Y. Watanabe, K. Ogata, and M. Kawai, Phys. Rev. C, **74**: 064613 (2006) [nucl-th/0611080]
109 J. Dabrowski and J. Rozynek, Phys. Rev. C, **78**: 037601 (2008)
110 J. Haidenbauer and U.-G. Meißner, Nucl. Phys. A, **936**: 29 (2015) [arXiv:1411.3114 [nucl-th]]
111 J. K. Ahn et al (KEK-PS E289 Collaboration), Nucl. Phys. A, **761**: 41 (2005)
112 J. K. Ahn et al (KEK-PS E-251 Collaboration), Nucl. Phys. A, **648**: 263 (1999)
113 M. Kohno, Y. Fujiwara, T. Fujita, C. Nakamoto, and Y. Suzuki, Nucl. Phys. A, **674**: 229 (2000) [nucl-th/9912059]